



OPEN Cycling with hemianopia to explore road user detection and scanning behaviour in virtual reality

E. M. J. L. Postuma¹, G. A. de Haan^{1,2}✉, F. W. Cornelissen³ & J. Heutink^{1,2}

Cyclists with homonymous hemianopia (HH) may face challenges in detecting road users, especially in unpredictable situations or with distractors. This study examined how HH affects detection, scanning behaviour, and the relation between detection and scanning in a virtual cycling environment.

Participants with real HH, simulated HH, and unimpaired vision (N = 12 per group) cycled in a virtual environment, braking upon detecting road users during predictable and unpredictable events, with and without distractors. Scanning behaviour and detection performance (time remaining at braking onset before a collision would have occurred (TTC)) were recorded.

TTC was similar across groups and unaffected by distractors. Real and simulated HH participants showed larger TTC declines, i.e. lower performance, during unpredictable events than unimpaired vision participants. Real HH participants scanned similarly to unimpaired vision participants, while simulated HH participants scanned their blind hemispace more. In real HH, wider horizontal gaze distribution was associated with longer TTC.

Individuals with HH can maintain detection performance in our virtual environment, but may be hindered more by unpredictability. Scanning a wider horizontal range may improve detection, but a scanning bias towards the blind hemifield, observed in simulated HH, did not.

Keywords Homonymous hemianopia, Road user detection, Scanning behaviour, Overt attention, Virtual reality

The timely detection of other road users is important for safe cycling. Yet, individuals with homonymous hemianopia (HH), who are deprived of perception in one half of their visual field due to acquired post-chiasmatic brain injury, may face considerable challenges in the timely detection and recognition of road users. Since a part of their peripheral vision is lost, they can miss cues that would normally trigger a gaze shift towards critical information, impairing their ability to direct overt attention. It has been found that some individuals with HH are less able to detect other road users when driving a car^{1–5}. Given the vital role of cycling in Dutch society, it is important to investigate how HH affects road user detection. Such research may aid in ensuring traffic safety, uphold the independence of individuals with HH, and promote their social participation.

To compensate for the loss of vision, individuals with HH may use scanning strategies that effectively allocate their gaze towards relevant visual information. When employing such effective scanning during driving, individuals with HH can achieve a road user detection performance comparable to those with unimpaired vision^{1,5}. Moreover, training individuals with HH to adopt a scanning strategy can decrease the impact of their visual field defect on mobility activities^{6,7}. Effective scanning may involve making larger saccades, frequent shifts between the left and right hemispaces, fewer central fixations, and scanning a wider visual range^{1,4,5,8}. Such effective scanning may differ from spontaneously adopted strategies, as the latter does not necessarily lead to similar task performance as those with unimpaired vision⁸. Despite its clear significance, the compensatory scanning strategies that may enable timely detection of road users in individuals with HH during cycling remain not well understood.

Environmental factors, such as the predictability of traffic situations or the presence of distractors, may influence the use of scanning strategies and thereby road user detection. For example, individuals may use contextual cues from their surroundings to guide eye movements⁹, suggesting that they may use anticipatory scanning at intersections to increase the likelihood of early road user detection. In this study, we define anticipatory scanning as changes in scanning behaviour in response to environmental cues that signal a

¹Department Clinical and Developmental Neuropsychology, Faculty of Behavioral and Social Sciences, University of Groningen, Groningen, The Netherlands. ²Royal Dutch Visio, Centre of Expertise for Blind and Partially Sighted People, Huizen, The Netherlands. ³Laboratory for Experimental Ophthalmology, University Medical Center Groningen, University of Groningen, Groningen, The Netherlands. ✉email: g.a.de.haan@rug.nl

potentially hazardous traffic situation. Previous research showed that experienced drivers, who used anticipatory scans more often than novices, showed a lower collision rate¹⁰. In contrast, at less predictable locations, such as hidden driveways or lawn pathways, road users may be detected later due to the absence of such anticipatory scanning. Additionally, distractors, such as billboards or a group of people conversing, may divert the gaze from relevant visual information, leading to delayed responses to hazardous road users while driving^{11–13}. Thus, to evaluate the effectiveness of compensatory scanning strategies in individuals with HH, it is essential to consider these environmental factors.

In this study, we aim to investigate whether the presence of HH influences road user detection and scanning behaviour during cycling in a virtual environment. This virtual environment has the potential to study road user detection and scanning behaviour in a standardised, controllable, and safe manner. We will compare individuals with real HH, unimpaired vision, and those with simulated HH. Including the simulated HH group may provide insights into the immediate impact of HH on road user detection and spontaneous changes in scanning, isolating the effects of the visual field defect itself from any comorbidities related to the acquired brain injury^{14,15}. Additionally, we will evaluate road user detection and scanning behaviour across predictable and unpredictable situations and in the presence or absence of environmental distractions. These findings may provide insights into the role of anticipatory scanning in road user detection and reveal how environmental distractions influence detection and scanning in individuals with HH. Lastly, to explore whether specific scanning strategies may be beneficial to road user detection, we will relate scanning behaviour to detection performance within each participant group and across event types.

To achieve these aims, we compared road-user detection, scanning behaviour, and their relationship across groups throughout the full cycling route, and specific to event types (see Fig. 1 for experimental set-up). Predictable events included the presence of an intersection (Fig. 1b), while unpredictable events took place without an intersection or side road present (Fig. 1c). A group of people, accompanied by the sound of chatter, served as a potential distractor (Fig. 1b). Road-user detection was measured by the time-to-contact, i.e., the time interval, in seconds, between the onset of braking and the estimated time of collision, had the participant not applied the brakes. Scanning behaviour was investigated by analysing the changes in horizontal gaze direction and gaze shift behaviour.

This study represents the first examination of road user detection and scanning in cyclists with HH in relation to different event types. The changes in scanning behaviour due to HH, the predictability of situations, and environmental distractors give insights into how overt attention is directed during cycling. Ultimately, it serves as an initial step towards optimising compensatory scanning training^{6,7} to increase safe cycling in individuals with HH in order to uphold their independence and promote their social participation.

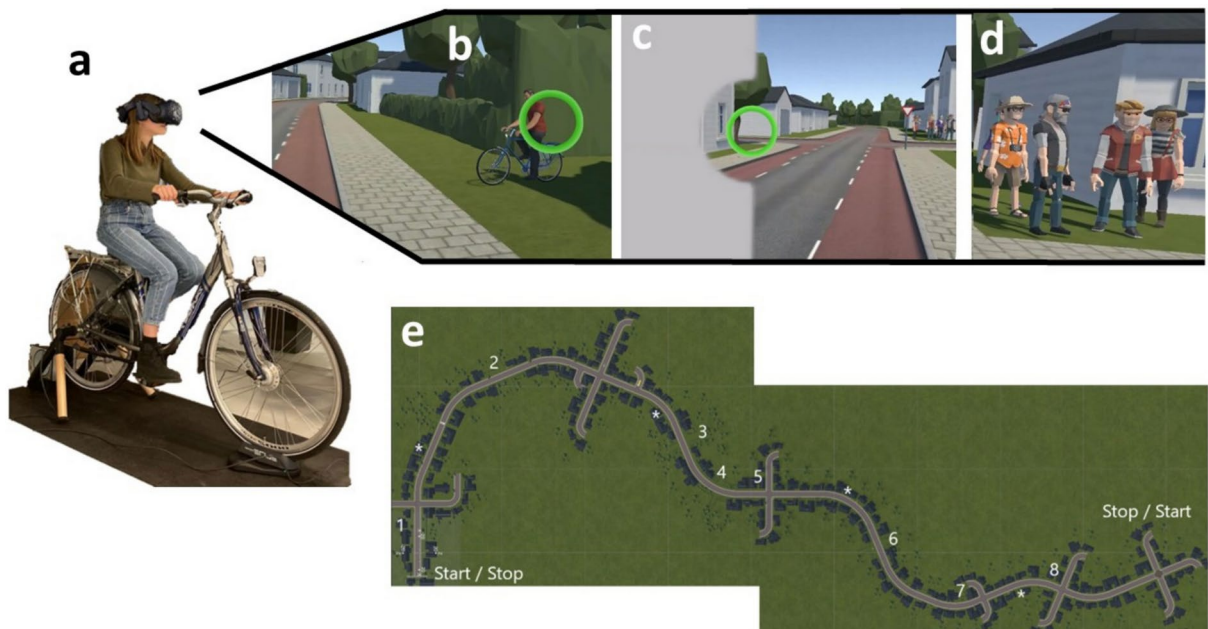


Fig. 1. The experimental set-up. The virtual (a) cycling simulator, (b–d) cycling environment from the viewers perspective, and (e) the cycling route. The cycling environment includes (b) unpredictable events (i.e. no intersection) and (c) predictable events (i.e. intersection present). At half of these events a distractor, i.e. a group of people talking, was present as is shown in figure c & d. Figure c provides an example of the simulation of homonymous hemianopia. The green circle in figure b–d indicates the gaze direction of the participant. The cycling route, as displayed in figure e, includes the start and stop location of the two cycling routes, and the events numbered in the order as presented in Table 4. The white asterisk marks locations where we included a group of people talking without any event occurring.

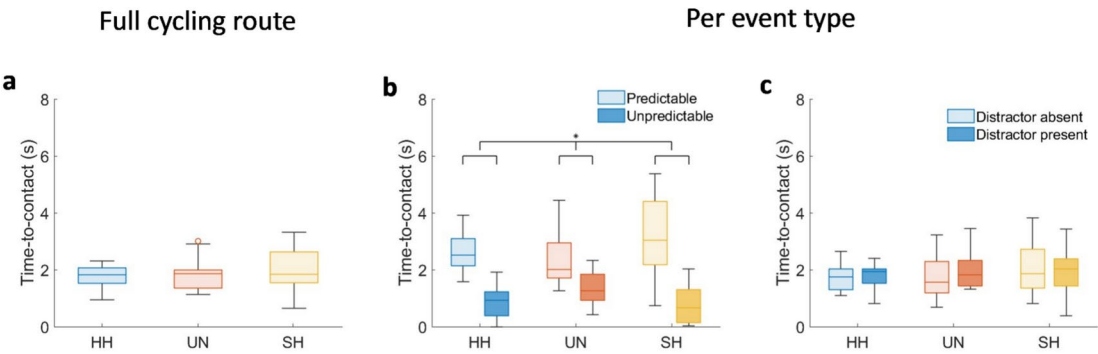


Fig. 2. Time-to-contact with other road users for the three groups during the full cycling route and per event type. Panel a shows, per group, the boxplots of the average time-to-contact across the full cycling route. Individuals with real HH (HH) are depicted in blue, individuals with unimpaired vision (UN) are illustrated in red, and individuals with simulated HH (SH) are demonstrated in yellow. Panel b shows, per group, the time-to-contact at predictable (light colours) and unpredictable (dark colours) events. The asterisk indicates a main effect of predictability and an interaction effect of the participant group by predictability (Table 1). Panel c shows, per group, the time-to-contact at events with a distractor absent (light colours) or present (dark colours).

		Time-to-contact (s)	Gaze in blind hemispace (%)	Horizontal gaze interquartile range (°)	Frequency of short gaze shifts (Hz)	Frequency of long gaze shifts (Hz)
Full route Participant-group ^a	F	0.492	23.790	1.559	0.722	0.885
	p	0.616	<0.001	0.227	0.494	0.423
	μ ²	0.029	0.613*	0.094	0.046	0.056
Predictability ^b	F	66.763	2.377	0.078	27.157	16.013
	p	<0.001	0.133	0.782	<0.001	<0.001
	μ ²	0.690*	0.067	0.002	0.451*	0.327*
Predictability * group ^b	F	3.576	1.322	0.269	0.068	0.009
	P	0.040	0.280	0.766	0.934	0.991
	μ ²	0.193*	0.074	0.016	0.004	0.001
Distractor ^b	F	0.362	5.592	0.057	0.901	0.037
	p	0.552	0.024	0.812	0.349	0.848
	μ ²	0.012	0.145*	0.002	0.027	0.001
Distractor * group ^b	F	1.356	0.383	1.016	0.961	0.339
	p	0.273	0.685	0.373	0.393	0.715
	μ ²	0.083	0.023	0.058	0.055	0.020
Full route TTC-group ^a	F	–	0.075	2.362	0.448	0.250
	p	–	0.785	0.135	0.508	0.621
	μ ²	–	0.002	0.073	0.015	0.008
Full route TTC-group * Participant-group ^a	F	–	2.181	3.373	0.558	1.714
	p	–	0.130	0.048	0.578	0.197
	μ ²	–	0.127	0.184*	0.036	0.103

Table 1. Full route and event-based statistical analysis comparing the road user detection and scanning behaviour across the participant groups. Significant results are presented in bold. *large effect sizes.–no analyses performed.

Results
The detection of road users

Figure 2 depicts the average time-to-contact across the full cycling route and per event type, i.e., predictable versus unpredictable events and events with a distractor absent versus present, across the three participant groups (real HH, unimpaired vision, and simulated HH). Figure A1 in the supplementary material a shows the number of collisions with other road users for the three groups during the full cycling route and per event type.

Overall, the three groups do not show any difference in their time-to-contact as indicated by the absence of a group main-effect and no large effect size (Fig. 2a, Table 1). The decline in the time-to-contact between

unpredictable compared to predictable events was larger for individuals with real and simulated HH compared to individuals with unimpaired vision (Fig. 2b). This is indicated by a main effect of predictability and an interaction effect of group by predictability with large effect sizes (Table 1). Post-hoc tests revealed that all groups decreased their time-to-contact significantly during unpredictable compared to predictable events ($p < 0.01$). It did not reveal a difference in the time-to-contact between the participant groups at the unpredictable events or predictable events ($p > 0.1$). The presence or absence of distractors did not influence the time-to-contact (Fig. 2c), indicated by the absence of both a main effect of the distractor and the interaction effect of the distractor by group.

Distribution of gaze direction during the full cycling route and per event type

Figure 3 depicts the horizontal gaze distribution during the full cycling route and per event type across the participant groups. Figure A2 in the supplementary material A illustrates the gaze direction variables used for statistical analysis during the full cycling route and per event type across the participant groups. First, it can be observed that, on average, the individuals with real HH and unimpaired vision more or less equally distributed their gaze over both hemispaces, whereas the individuals with simulated HH distributed their gaze more towards their blind hemispaces. This observation is supported by a higher percentage of gaze directed towards the blind hemispaces in the simulated HH group compared to the other two groups, as is indicated by a group main-effect

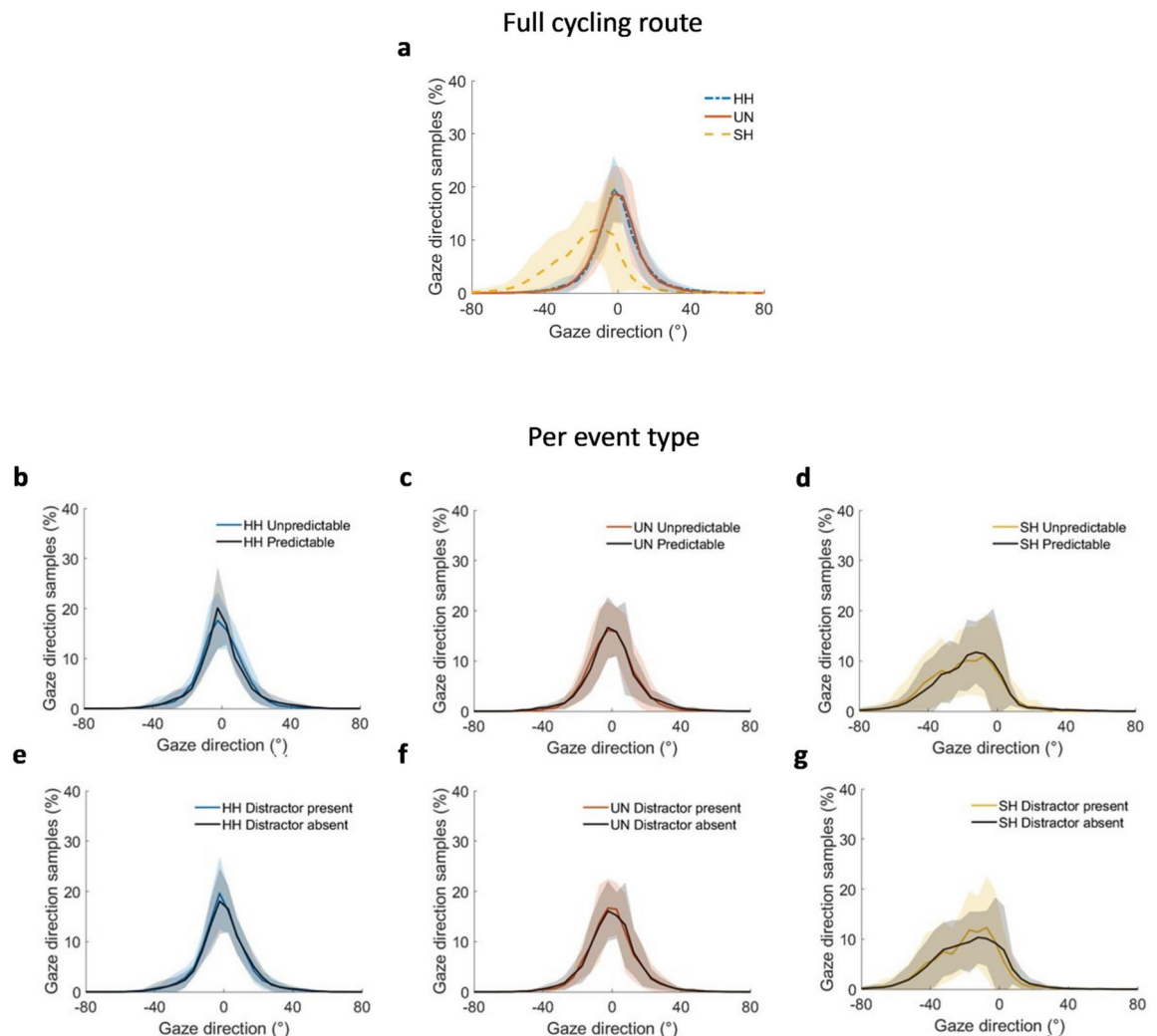


Fig. 3. Comparison of horizontal gaze direction distribution during the full cycling route and per event-type across participant groups. Panel (a) shows the distribution of the horizontal gaze for each participant group. Individuals with real HH (HH) are depicted in blue, individuals with unimpaired vision (UN) are illustrated in red, and individuals with simulated HH (SH) are demonstrated in yellow. Panel (b–d) shows the distribution of the horizontal gaze during unpredictable and predictable events for each participant group. Panel (e–g) shows the distribution of the horizontal gaze at events with a distractor present and absent events for each participant group. A negative gaze direction indicates that the gaze is directed to the blind hemispaces, whereas positive values indicate a gaze direction towards the visible hemispaces. The coloured areas indicate the standard deviations for each participant group.

with a large effect size (Table 1, Fig. 3a). The participants' groups do not differ in their range of horizontal gaze (i.e., no group main-effect with large effect size for horizontal gaze interquartile range).

None of the participant groups show much difference in their distribution of horizontal gaze between predictable and unpredictable events (Fig. 3b–d). This is supported by no difference in the percentage of gaze allocated to the blind hemispace nor in the interquartile range of the horizontal gaze (i.e. no main-effect of predictability or an interaction effect of predictability by group interaction-effect).

When distractors are present, the participants' groups also do not show much difference in their distribution of horizontal gaze compared to when distractors are absent (Fig. 3e–g). There was a statistically significant effect, suggesting an increase in the percentage of gaze in the blind hemispace when distractors are present compared to absent (i.e., a main-effect of the distractor). However, this increase is negligibly small (3.0%) and did not differ across groups, indicated by an absence of an interaction effect of distractor by group. The presence of distractors did not influence the interquartile range of the horizontal gaze (i.e., no main-effect of predictability or an interaction effect of predictability by group).

Gaze shift behaviour during full cycling route and per event type

Figure 4 depicts the gaze shift behaviour during the full cycling route and per event type across the participant groups. Figure A3 in the supplementary material A illustrates the gaze shift variables used for statistical analysis during the full cycling route and per event type across the participant groups. No difference in gaze shift behaviour across groups during the full cycling route can be observed (Fig. 4a), supported by the absence of differences in the frequency of long and short gaze shifts across groups (i.e., no group main-effect, Table 1).

It can be observed that at unpredictable events all three participant groups show a higher frequency of gaze shifts with an amplitude between 5 and 15 degrees compared to predictable events (Fig. 4b–d). This pattern resulted in an increased frequency of short gaze shifts at unpredictable events compared to predictable events, which was similar across groups (i.e., main-effect of predictability with a large effect size and the absence of an interaction effect of predictability by group, Table 1). Additionally, a decrease in the frequency of long gaze shifts was found for unpredictable events compared to predictable events, which was also similar across groups (i.e., main-effect of predictability with a large effect size and the absence of an interaction effect of predictability by group, Table 3). Note, that these differences in the frequency of short and long gaze shifts are minimal, 0.11 and 0.03 Hz respectively.

The participant groups do not deviate much in their gaze shift behaviour when a distractor is present or absent (Fig. 4e–g). Nor were there any differences found in the frequency of short and long gaze shifts between events with and without a distractor present across groups (i.e. no main-effect of the distractor nor a distractor by group interaction effect, Table 1).

Distribution of gaze direction in relation to road user detection

Figure 5a–c illustrates the differences in gaze direction during the full cycling route between individuals with long and short time-to-contact. The gaze direction variables in relation to the time-to-contact are illustrated in Figure A4a–d (for the full cycling route) and Figure A5 and A6 (per event type) in the supplementary material A.

During the full cycling route, it can be observed that individuals with real HH and a long time-to-contact show a broader range in their horizontal gaze distribution with the peak distribution slightly closer to the centre compared to those with real HH and a short time-to-contact (Fig. 5a). This was not observed in those with unimpaired vision (Fig. 5b) and those with simulated HH (Fig. 5c). The observed pattern is supported by an increase in the interquartile range of horizontal gaze in those with a long time-to-contact compared to a short time-to-contact in only the real HH group during the full cycling route (i.e., interaction-effect of TTC by group with a large effect size; Table 1). Additionally, only in the HH group, a strong positive correlation was found between the time-to-contact and the horizontal gaze interquartile range during the full cycling route (Table 2). This strong positive correlation between the time-to-contact and the horizontal gaze interquartile range in individuals with real HH was also found when a distractor was absent, but not at predictable events, unpredictable events, or when a distractor was present (Table 2).

Gaze shift behaviour in relation to road user detection

Figure 5, panels d–f, illustrate the differences in gaze shift behaviour during the full cycling route between individuals with long and short time-to-contact. The gaze shift variables in relation to the time-to-contact are illustrated in Figure A4e–h (for the full cycling route) and Figure A7 and A8 (per event type) in the supplementary material A. Individuals with real HH and a long time-to-contact show a small increase in gaze shift with an amplitude between 35 and 55 degrees compared to those with real HH and a short time-to-contact (Fig. 5d). This difference did not result in significant differences in the frequency of long gaze shifts between individuals with a long and short time-to-contact across groups during the full cycling route (i.e., no TTC main-effect or an interaction effect of TTC by group, Table 1). There was a significant and strong positive correlation between the frequency of long gaze shifts and the time-to-contact in the real HH group during the full cycling route (Table 2). This strong positive correlation between the time-to-contact and the frequency of long gaze shifts in individuals with real HH was also found when a distractor was absent, but not at predictable events, unpredictable events, or when a distractor was present (Table 2).

Individuals with unimpaired vision and a long time-to-contact showed a small increase in gaze shifts with an amplitude between 5 and 15 degrees compared to those with unimpaired vision and a short time-to-contact (Fig. 5e). We did, however, not find a significant difference in the frequency of short gaze shifts between individuals with a long and short time-to-contact across groups during the full cycling route (i.e., no TTC main-effect or an interaction effect of TTC by group, Table 1). Additionally, the frequency of short gaze shifts did not

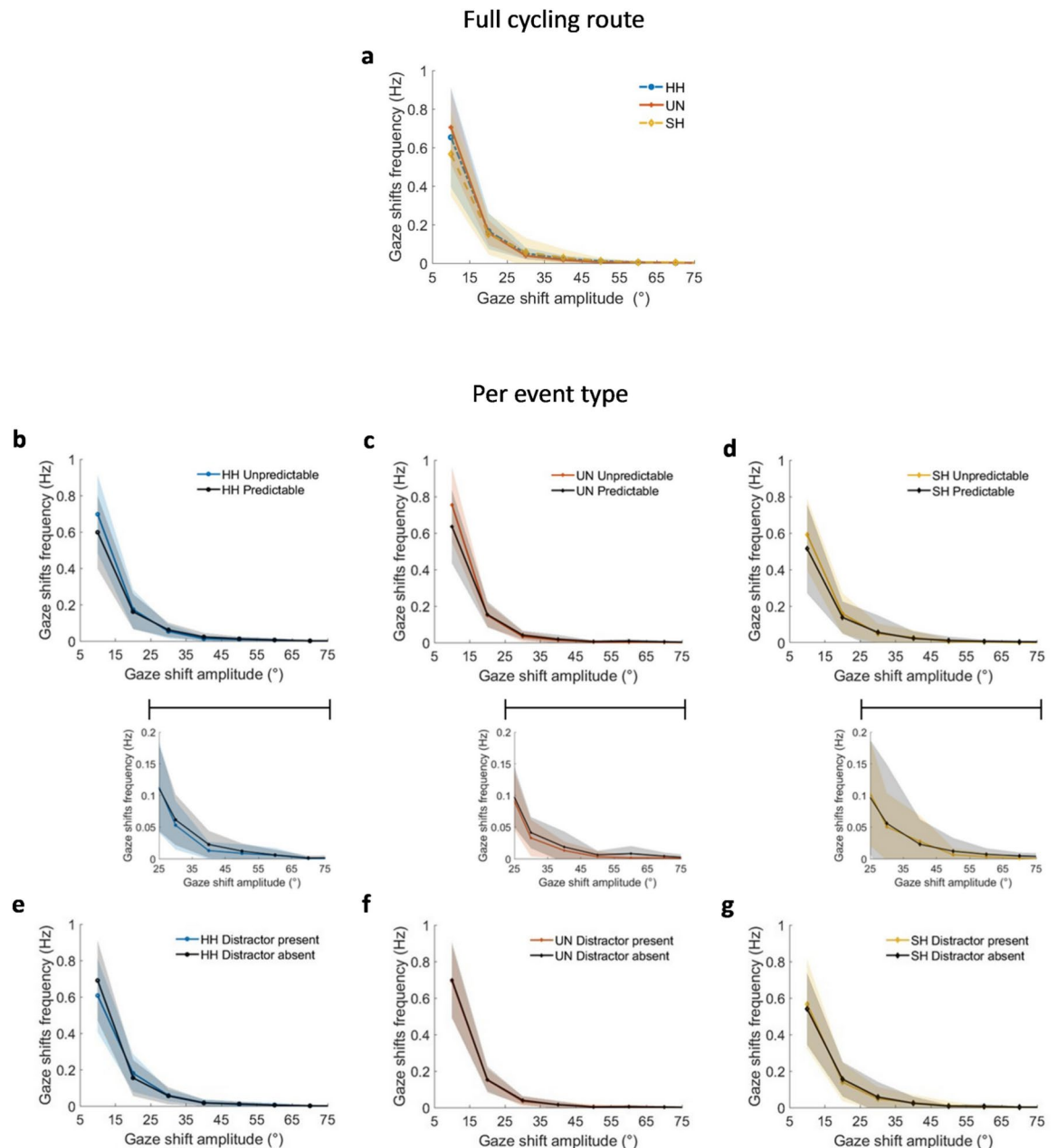


Fig. 4. Comparison of gaze shift behaviour during the full cycling route and per event-type across participant groups. Panel (a) shows the gaze shift frequency per gaze shift amplitude, which is divided in bins of 5 degrees. Individuals with real HH (HH) are depicted in blue, individuals with unimpaired vision (UN) are illustrated in red, and individuals with simulated HH (SH) are demonstrated in yellow. Panel (b–d) shows the gaze shift frequency per gaze shift amplitude during unpredictable and predictable events for each participant group, with a zoom in on long gaze shifts (25–75 degrees). Panel (e–g) shows the gaze shift frequency per gaze shift amplitude at events with a distractor present and absent events for each participant group. Short gaze shifts are defined as gaze shifts with an amplitude below 25 degrees whereas long gaze shifts are defined as gaze shifts with an amplitude above 25 degrees.

strongly correlate with the time-to-contact in each group during the full cycling route or at a specific event (Table 2).

Discussion

This study yields four key findings regarding the detection of road users and the scanning behaviour of individuals with HH when cycling in a virtual environment. First, HH defects, whether real or simulated, did not impair the overall ability to detect road users compared to individuals with unimpaired vision, nor was it influenced by the presence of distractors. Second, all groups show a lower detection performance at unpredictable

Full cycling route

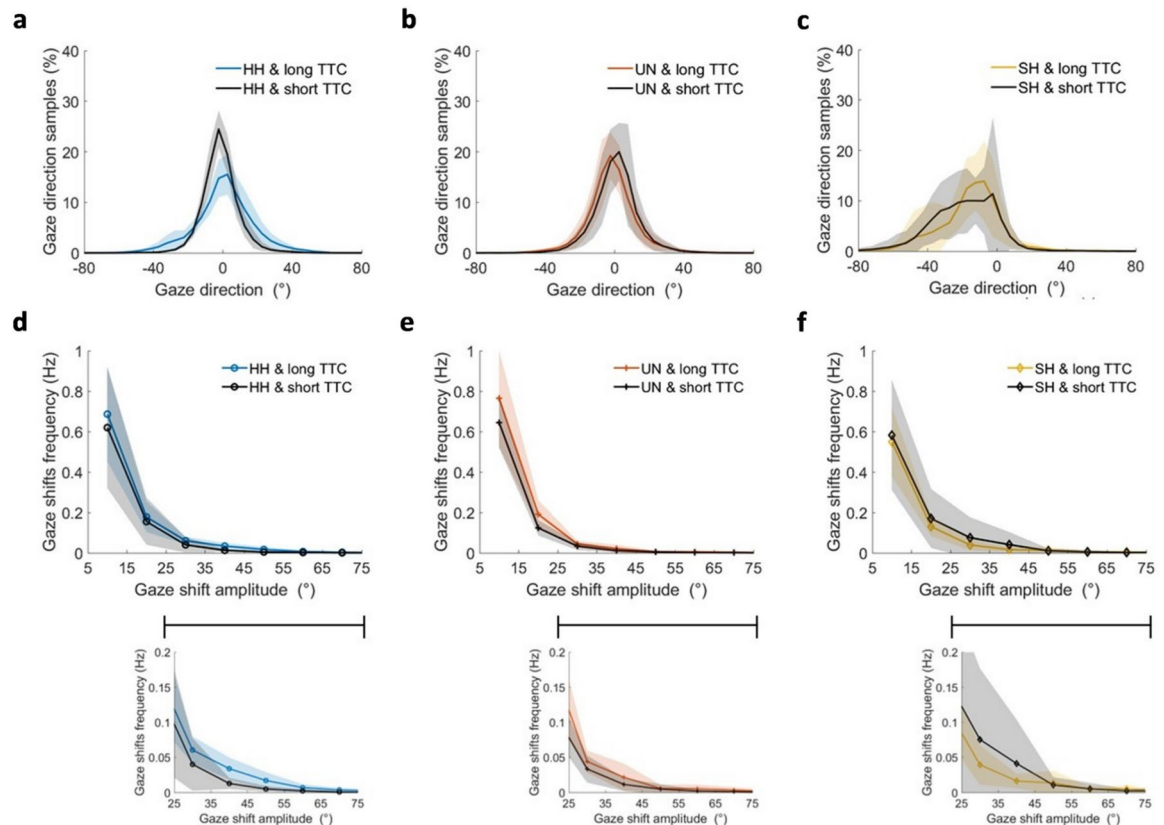


Fig. 5. Comparison of gaze direction distribution and gaze shift behaviour during the full cycling route between individuals with a long and short time-to-contact. Panel (a–c) shows the distribution of the horizontal gaze for individuals with a long and short time-to-contact within each participant group. Individuals with real HH (HH) are depicted in blue, individuals with unimpaired vision (UN) are illustrated in red, and individuals with simulated HH (SH) are demonstrated in yellow. A negative gaze direction indicates that the gaze is directed to the blind hemispace, whereas positive values indicate a gaze direction towards the visible hemispace. Panel (d–f) shows the gaze shift frequency per gaze shift amplitude for individuals with a long and short time-to-contact within each participant group. The gaze shift amplitude is divided into bins of 5 degrees with Short gaze shifts defined as gaze shifts with an amplitude below 25 degrees and long gaze shifts defined as gaze shifts with an amplitude above 25 degrees. The inserts below panels d–f zoom in on the Larger amplitude sections of the panels.

events compared to predictable events, however individuals with real and simulated HH were more hindered by the unpredictability compared to the unimpaired vision group. Third, in general, the scanning behaviour of individuals with real HH did not differ from that of those with unimpaired vision. In contrast, those with simulated HH directed their gaze more towards the blind hemispace than those with real HH and unimpaired vision. Last, specific scanning patterns might improve detection performance. Among individuals with real HH, we observed that wider horizontal gaze distribution related to a better detection performance. Below, we discuss these findings and conclusions in more detail.

In this study, individuals with real or simulated HH demonstrated a similar road user detection performance during cycling as those with unimpaired vision. The detection performance was not influenced by the presence of a distractor. Additionally, we only observed a minimal change in scanning behaviour due to the presence of distractors. These findings contrast with previous studies^{11–13}, possibly due to billboards being more distracting than the group of people conversing used in our study. Nevertheless, within our current virtual environment, all participant groups were highly visually attentive to the task, as they maintained consistent detection performance despite the presence of distractors.

Unlike the presence of distractors, the predictability did influence road user detection. All groups showed lower detection performance during unpredictable events compared to predictable ones, with individuals experiencing HH being more hindered by the unpredictability. This suggests that HH can profit from predictability to maintain their detection performance, whereas unpredictability may increase collision risk in individuals with HH. It remains unclear whether anticipatory scanning contributed to the better detection performance in predictable events. Individuals employed fewer short but more long gaze shifts during predictable events. This might imply that individuals perform more goal-directed gaze shifts during predictable events compared

		Gaze in blind hemispace (%)		Horizontal interquartile range (°)		Frequency of short gaze shifts (Hz)		Frequency of long gaze shifts (Hz)	
		r	p	r	p	r	p	r	p
Throughout full cycling route	HH	−0.361	0.249	0.568	0.054	0.08	0.805	0.643	0.024
	UN	0.446	0.146	0.079	0.807	0.390	0.210	0.220	0.492
	SH	0.028	0.932	0.096	0.766	0.271	0.394	−0.04	0.991
Unpredictable	HH	−0.031	0.923	0.559	0.059	0.242	0.499	0.401	0.197
	UN	0.369	0.238	0.274	0.389	0.308	0.329	0.295	0.351
	SH	−0.209	0.515	−0.003	0.993	−0.171	0.596	−0.091	0.779
Predictable	HH	−0.135	0.677	−0.061	0.850	−0.391	0.209	0.346	0.270
	UN	0.294	0.354	−0.096	0.766	0.155	0.630	0.107	0.741
	SH	0.201	0.531	0.486	0.109	0.418	0.177	0.177	0.582
Distractor present	HH	−0.380	0.223	0.230	0.472	0.047	0.884	0.426	0.167
	UN	0.237	0.458	0.067	0.837	0.179	0.578	0.385	0.217
	SH	0.307	0.332	0.363	0.246	0.332	0.292	0.217	0.498
Distractor absent	HH	−0.485	0.110	0.536	0.072	−0.105	0.745	0.434	0.159
	UN	0.502	0.096	0.046	0.888	0.331	0.294	0.187	0.562
	SH	0.039	0.904	0.464	0.128	0.225	0.482	−0.31	0.923

Table 2. Correlation analysis between the time-to-contact and the scanning behaviour. Strong correlations are presented in bold.

to explorative small gaze shifts during unpredictable events. Yet, these changes in gaze shift behaviour were relatively small. Moreover, we did not find related changes in horizontal gaze direction. Alternatively, individuals may have opted for anticipatory strategies beyond scanning behaviour (e.g. adapting their speed) that improved their detection performance at predictable events compared to unpredictable events.

We identified scanning behaviour that might improve the detection performance of individuals with HH. A wider horizontal gaze distribution may be associated with a better detection performance, particularly during events without distractors. These findings align with a previous driving study showing that a wider horizontal distribution of fixations was linked to a better detection of objects on a collision course without intersections present¹. Next to a wider horizontal gaze distribution, we observed that a higher frequency of larger gaze shifts might relate to a better detection performance. While these long gaze shifts occur rather rarely, performing just one or two of these long gaze shifts might be crucial for detecting other road users. Yet, the current results are inconsistent, showing a strong overall correlation in individuals with real HH, but not when comparing those with a high or low detection performance, making it impossible to draw definitive conclusions.

The relationship between detection performance and scanning emerged only in the absence of distractors. Without distractors, individuals with HH may be more impeded in making long gaze shifts or expanding their horizontal gaze distribution, as fewer external cues prompt them to do so. Performance then depends more on pro-active employment of scanning strategies, revealing differences in scanning behavior, particularly because some individuals with HH may not actively scan their environment. However, given the limited data, these findings should be interpreted with caution.

Individuals may employ compensatory strategies beyond scanning in predictable situations. In our experiment, we observed that participants tended to brake more frequently before hazardous road users appeared in the scene during predictable events compared to unpredictable ones (see supplementary material D). This behaviour likely reflects tactical compensation, where actions are taken in anticipation of upcoming traffic situations¹⁶. Previous research suggests that individuals with vision loss often reduce cycling speed as a form of tactical compensation¹⁷. Although our study did not account for speed adjustments, this frequent braking may have served as a preparatory action to reduce cycling speed in anticipation of a critical event.

In general, individuals with real HH did not show compensatory scanning compared to those with unimpaired vision. Individuals with simulated HH, on the other hand, directed their gaze more toward their blind hemifield than those with real HH and unimpaired vision. This focus on the blind hemispace aligns with findings from search and driving tasks in both individuals with real and simulated HH^{2,14,15,18,19}. The absence of such bias in our real HH group may be attributed to individuals who began or completed a compensatory scanning training, focussing on making long eye-movements to both the blind and visible hemispace^{6,7}. Consequently, individuals with simulated HH seem to exhibit more spontaneous adaptation, while real HH participants, accustomed to long-term vision loss and possible training, do not. Alternatively, simulated HH participants might exaggerate compensatory scanning due to heightened awareness of their induced deficit.

Interestingly, the bias towards the blind hemispace was not related to improved detection performance in individuals with either real and simulated HH. This suggests that the bias towards the blind hemispace could represent spontaneous compensatory scanning strategy that does not enhance detection performance. Indeed, previous driving studies have shown that individuals with HH may adopt such bias², while it is not found to relate to a better driving performance^{1,5,8,20}.

Our findings provide insights into the deployment of overt attention during cycling, showing that individuals are not easily distracted by environmental factors and increase their attention to road users at predictable events. Even individuals with HH, despite a restricted visual field, maintain their detection performance in such situations. To respond in a timely manner to road-users, individuals with HH may benefit from allocating their gaze to a wider horizontal range. This might require a top-down gaze allocation strategy, as their gaze shifts are less guided by peripheral input. Lastly, a spontaneous attentional bias towards the blind hemispace does not seem to aid road user detection.

Our study has various limitations. The drop-out rate due to simulator sickness was high, 25%, affecting four real HH, three unimpaired vision, and five simulated HH participants. However, simulator sickness did not seem to affect the detection performance or the scanning behaviour in the remaining 36 participants (see supplementary material C). The recorded data per event type was limited, i.e. 1.7–1.9 min per participant. This short time frame was chosen to ensure that the scanning behaviour data was specifically related to the upcoming event, rather than earlier events or not event-related scanning. Additionally, we included data on scanning behaviour during the full cycling route, which had an average duration of 8.7 min per participant. With 12 participants per group, data for correlation analysis was limited. We used non-parametric methods to examine the link between detection performance and scanning behaviour, noting that parametric analysis would yield different results (see supplementary material E). Further research is needed to generalise these findings. The average data loss per participant during the full cycling route and event-based was low, i.e., 3.8–5.8%. Our calibration check showed no differences in accuracy between participant groups. For more information on the data quality, see supplementary material B.

In the second route, the events were repeated in reverse order, potentially reducing the unpredictability of unpredictable events. However, the participants were not informed about the repetitions of events. The decrease in time-to-contact during the second route was similar between unpredictable (0.43 s) and predictable events (0.46 s). Therefore, it seems unlikely that repeating the events influenced the unpredictability of unpredictable events. See supplementary material F for more information.

The eye- and head-tracking system operated at a relatively low sampling rate of 40 Hz, likely due to the high CPU demands of the virtual cycling simulator. In contrast, our virtual reality setup without the cycling simulator attached achieved a higher sampling rate of 90 Hz²¹. This lower sampling rate impacted the gaze shift classifier, reducing its ability to classify gaze shifts with an amplitude below 5 degrees. These small gaze shifts were not critical for answering our main research questions and were therefore excluded from our analysis. As a result, we do not expect the low sampling rate to have significantly affected our findings. In addition to the limited ability to classify gaze shifts with amplitudes below 5 degrees, small gaze shifts may have been misclassified during high-noise phases caused by body movements due to the variable velocity threshold of the gaze shift classifier. We do not, however, expect that the choice of the classifier would significantly impact the observed differences in scanning behaviour across participant groups and event-type.

The head-mounted display had a limited field of view. This may have reduced road user detection across all participants groups²². If so, this may primarily have affected the unpredictable events. Moreover, the restricted field of view may have altered scanning behaviour by inducing more head movements with larger amplitudes and a smaller range of eye position^{23–25}. To limit this effect, we focused on gaze direction and shifts, omitting separate analyses of head and eye movements. Lastly, individuals may have been less likely to perform long gaze shifts due to the inability to respond to peripheral input caused by the restricted field of view. Since all groups experience this limitation, we expect the effect to be similar across groups.

Overall, our results should be interpreted relative to participant groups, event types, and time-to-contact within our specific setup and virtual experiment, rather than as directly reflecting real-life behaviour. For example, in our study, steering was not required and did not influence position on the road, allowing participants to focus on the virtual environment without needing to adapt to complex cycling operations in virtual reality. This may have affected the road user detection performance results. Previous work found that individuals with HH were less able to detect moving objects while navigating a parcourse by walking compared to sitting on a chair²⁶. Similarly, individuals with HH may face more difficulties with road user detection during cycling, while they also must navigate the cycling path. This would coincide with alterations in scanning behaviour, as they need to use their vision to navigate cycling paths. The constant speed in our study could have hindered road-user detection, as individuals could not slow down near intersections. Slowing down would allow for increased time to visually scan the traffic situations. Still, we did observe more frequent braking at predictable compared to unpredictable events, suggesting a preparatory action to reduce cycling speed in anticipation of a critical event.

Our study is among the first to investigate both road user detection and scanning behaviour during cycling in a clinical population. By linking detection performance to scanning behaviour and examining the effects of predictability and distractors, it provides insights into the deployment of overt visual attention during a daily-life task. However, with its various limitations in mind, we want to emphasise that the results of this study should not yet be considered generalisable to clinical contexts but rather as pioneering work that lays the groundwork for future studies. These future studies could use advancements in cycling simulators to determine whether our findings hold when individuals with HH must maintain lane position and stability. Additionally, introducing distractors, such as moving pedestrians or billboards, could further assess the impact of task-irrelevant distraction.

In this study, we provided the first insights on road user detection and scanning behaviour in individuals with HH while cycling in a virtual environment. The key findings show that individuals with real and simulated HH maintained their road user detection performance and visual scanning patterns despite the presence of distractors. Road-user detection was better in anticipation of an intersection than at unpredictable events, with individuals with HH being more hindered by the unpredictability than those with impaired vision. Individuals with HH might be able to improve road user detection by adopting a wider horizontal gaze distribution. Lastly,

individuals with simulated HH showed a scanning bias towards their blind hemifield, potentially indicating a spontaneous scanning strategy that may not lead to a better detection performance. Future research should investigate whether individuals with HH use tactical compensation by reducing cycling speed and whether this strategy may improve road user detection. Additionally, the role of anticipatory scanning behaviour when approaching intersections warrants further investigation, as well as the relationship between scanning behaviour and detection performance in the presence or absence of distractors and intersections. It also offers insights into the deployment of overt visual attention during a daily-life task. Our study is a first step in understanding road-user detection and cycling behaviour in individuals with HH. Advancements in cycling simulators should help confirm whether our findings hold under the requirements of maintaining lane position and stability, or with stronger distractors, such as moving pedestrians or billboards.

Method
Participants

This study enlisted a total of 48 participants, comprising 16 individuals with real HH, 15 individuals with unimpaired vision, and 17 individuals with unimpaired vision for which HH was simulated. A total of twelve participants were unable to finish the study due to simulator sickness, consisting of four individuals with real HH, three individuals with unimpaired vision, and five individuals with simulated HH. Of the remaining participants with real HH, five experienced right HH and seven experienced left HH. Detailed demographic information about the remaining participants is provided in Table 3.

Individuals in the real HH group were recruited via Royal Dutch Visio, centre of expertise for visually impaired and blind people, while the age- and gender-matched participants with unimpaired vision and simulated HH were recruited through social media advertisements. Individuals with HH were checked for inclusion by data provided during their screening process as part of their regular intake at Royal Dutch Visio. Individuals within the unimpaired vision and simulated hemianopia group provided self-reported data through a questionnaire. The inclusion criteria for all participants were age ≥ 18 years, self-reported normal or corrected to normal vision, and a Mini-Mental State Examination score of 24 or higher²⁷, no impairments in eye or head motility, no psychiatric disorders, no evident impairments in the following domains: memory, attention (such as neglect), language and communication, balance, and orientation. Specific inclusion criteria for the HH group included a homonymous visual field defect of at least quadrantanopia level with a neurological cause and the absence of any visual field defect on the ipsilesional side, a minimum duration of 3 months since the onset of hemianopia, and a binocular visual acuity of Snellen ≥ 0.5 (6/12 or 20/40, logMAR 0.3). Lastly, the clock drawing test was administered among individuals with HH at the start of the experiment to further check for symptoms of neglect.

Informed consent was obtained from all participants, and the study received ethical approval from the medical ethical committee of the Medical University Centre of Groningen (NL72491.042.20). The study was

Participant group (N)	HH (12)	UN (12)	SH (12)
Age in years (mean (SD) [range])	58 (19) [22–80]	58 (19) [22–82]	60 (21) [20–79]
Gender (male in % (N))	83.3 (10)	83.3 (10)	83.3 (10)
Cause of HH (% (N))			
Stroke	66.7 (8)	–	–
Traumatic brain injury	25.0 (3)	–	–
Tumour	8.3 (1)	–	–
Side of HH (right % (N))	41.7 (5)	–	41.7 (5)
Size of HH (% (N))			
Homonymous hemianopia	75.0 (9)		75.0 (9)
Quadrantanopia	25.0 (3)	–	25.0 (3)
Macular sparing > 5° (Yes in % (N))	50.0 (6)	–	50.0 (6)
Time since onset in months (mean (SD) [range])	25.2 (16.4) [7–58]	–	–
Completion compensatory scanning training (% (N)) ^a			
Stage 0	16.7 (2)	–	–
Stage 1	8.3 (1)	–	–
Stage 2	0 (0)	–	–
Stage 3	8.3 (1)	–	–
Finished	41.7 (5)	–	–
No training necessary ^b	25.0 (3)	–	–

Table 3. Demographic information of the three participants groups. Compensatory scanning training of Royal Dutch Visio6,7, Stage 0: training did not start, Stage 1: practising scanning while walking inside, Stage 2: practising scanning while walking outside, Stage 3: practising scanning while cycling outside. No training necessary according to the occupational therapist HH: participants with real homonymous hemianopia. UN: participants with unimpaired vision. SH: participants with simulated homonymous hemianopia.

Event	Approaching side	Predictability	Distractor
1	Right	Predictable	Absent
2	Right	Unpredictable	Present
3	Right	Unpredictable	Absent
4	Left	Unpredictable	Absent
5	Left	Predictable	Present
6	Left	Unpredictable	Present
7	Left	Predictable	Absent
8	Right	Predictable	Present

Table 4. Events with approaching cyclists.

performed according to the Declaration of Helsinki. The participants also took part in another study investigating compensatory behaviour while crossing streets²¹.

Apparatus

The HTC Vive Pro Eye (HTC Corporation, Toayuan, Taiwan) displayed the virtual cycling environment and features a sampling rate of 40 Hz and a resolution of 1440 × 1600 pixels. The world view was 360°. The field of view of the head-mounted display was approximately 90° horizontally and vertically. The head-mounted display included an adjustable headphone, which was used to deliver audio sound to the participants. The HTC Vive Base Stations (HTC Corporation, Toayuan, Taiwan) captured the head rotation, while the built-in eye tracker (Tobii XR) collected the eye-orientation data. This eye-orientation data was accessed through the software Vive SRanipal SDK (HTC Corporation, Toayuan, Taiwan) at a sampling rate of 40 Hz. The eye tracker required a 5-point calibration and, according to the manufacturer, provided an accuracy of 0.5–1.1 degrees.

The bicycle resembled bicycles commonly used in the Netherlands (Fig. 1a). A low-entry bicycle equipped with hand brakes was selected for this study. The bicycle’s rear wheel was mounted on an Elite Tuo bicycle trainer (Elite, Fontaniva, Italy), which monitored whether the participants were cycling. The bicycle’s hand brakes were connected to an HTC Vive controller (HTC Corporation, Toayuan, Taiwan) to serve as a button press sensor for detecting the brake application. When the brakes were applied, the cycling velocity was rapidly reduced to zero to minimise the participants’ exposure to perceptual mismatches (i.e., visual deceleration without corresponding physical forces), thereby reducing simulator sickness. To ensure precise timing of the potential collision with the virtual road users, participants maintained a constant cycling speed (14 km/h) throughout the experiment. This precise timing was essential, as it required individuals to brake to avoid collisions with oncoming cyclists, making braking a reliable measure of road-user detection. Steering was possible but not required and did not influence position on the road, allowing participants to focus on the virtual environment without needing to adapt to complex cycling operations in virtual reality. It should be noted that in real-life, steering can negatively affect road-user detection and alter scanning, as individuals also need to use their vision to navigate cycling paths. Adjusting speed could, however, have a positive effect on road-user detection, as they may be able to anticipate oncoming traffic when approaching an intersection by slowing down.

The development of the virtual cycling environment in Unity (Unity Technologies, San Francisco, USA) was outsourced to The Virtual Dutch Men Corporation (Almelo, The Netherlands) and based on specifications provided by the authors. The simulation represented an urban setting, featuring two red bicycle lanes on either side of a central car lane, lined with trees, hedgerows, and suburban houses (Fig. 1b–e). While cycling, participants encountered approaching cyclists on a collision course from the left or right side, cycling with a speed of 12 km/h (Table 4 and Fig. 1b–d). When the cyclist on a collision course appeared on the scene, the angle between the participant’s heading and the virtual cyclist ranged from 45 to 50 degrees. The angle varied depending on whether the virtual cyclist approached from the left or right, as participants were always cycling in the right lane. If a collision occurred between the participant and an approaching cyclist, the cyclist would disappear. These road users could appear at crossroads (i.e., predictable events; Fig. 1c) as well as at locations without a side road present (i.e., unpredictable events; Fig. 1b). At half of these events, a group of people was presented (Fig. 1c–d), accompanied by the sound of chatter delivered through the headphones, serving as potential distractors. This group of people was also present four times along the cycling route when there was no event taking place (Fig. 1e). Additionally, a pedestrian crossed between events 1 and 2, a car crossed between events 2 and 3, and a truck drove in the opposite direction between events 2 and 3. These events were included for evaluation of the cycling simulator within clinical practice but were not analysed in this study.

The hemianopia simulation was developed by The Virtual Dutch Men Corporation (Almelo, The Netherlands), using Unity (Unity Technologies, San Francisco, USA). The simulation featured a grey area with a clear boundary between the visible and blind parts of the visual field, which was superimposed on the head-mounted display (Fig. 5c). The size and position of the grey area were customised for each individual with simulated HH, replicating the visual field of their age- and gender-matched counterpart with HH. The simulation dynamically adjusted to the participant’s eye position, based on the data provided by the built-in eye tracker.

To monitor and safeguard the well-being of the participants, the Misery Scale²⁸ was employed to conclude the experiment if severe nausea symptoms occurred. The Misery Scale is an 11-point scale that assesses varying levels of nausea symptoms. A score above 6 would indicate severe nausea symptoms, signalling the termination of the experiment.

The Simulator Sickness Questionnaire²⁹ was used to assess the participant's simulator sickness after completion of the cycling route. This questionnaire consists of 16 items rating the simulator sickness symptoms with the subscales oculomotor discomfort, disorientation, and nausea. The severity of the symptoms is rated by a four-point Likert scale ranging from not to severely experiencing the symptoms. For outcomes on the simulator sickness questionnaire, see supplementary material C.

Procedure

The experiment was conducted at multiple Royal Dutch Visio rehabilitation centres (in Haren, Leeuwarden, Rotterdam, Nijmegen, and Amsterdam). At the start of the experiment, the participants were seated on the bicycle and fitted with the head-mounted display. The headset, equipped with a built-in eye tracker, was then calibrated, and the audio system was checked for proper functionality. Following calibration, a calibration check was performed that required the participant to sequentially direct their gaze towards predefined locations in the VR environment. Prior to the experimental phase, participants familiarised themselves with the braking mechanism of the cycling simulator by stopping at designated stop signs along a traffic-free cycling route. Once the familiarisation period was complete, the experimental phase began. Participants were instructed to respond to crossing road users approaching from either the left or right side by using the hand brakes in a timely manner. The first cycling route consisted of the eight events described in Table 4, following an ascending order from 1 to 8. For the second route, the participants cycled the same path in the opposite direction, encountering the events in descending order from 8 to 1. Participants could not adjust their cycling speed except by braking, which always resulted in a rapid deceleration of the cycling velocity to zero. Additionally, steering was not required to follow the cycling route. The Misery scale was administered after the completion of the practice round and after the completion of the first cycling route (i.e., encountering the events in Table 4 in ascending order). Participants were only allowed to continue if their MISC score was 6 or lower. The simulator sickness questionnaire was administered after completion of the second cycling route. For outcomes on the simulator sickness questionnaire, see supplementary material C.

Data analysis

The head and eye-tracking data were analysed using MATLAB (v2022b; The MathWorks Inc., Natick, MA, USA). The head orientation data was originally recorded in the virtual world reference frame, meaning it captured not only the participant's head movements but also rotations caused by the direction of the cycling route. To isolate the participants' head movements, we subtracted the cycling route's rotation from the head rotation data, converting the head rotation to a body-centred reference frame. The eye-tracking data, obtained by the built-in eye tracker, consisted of normalised eye-orientation vectors with values ranging from -1 to 1 ³⁰. To ensure high data quality, the validity measure provided by the eye tracker was used to exclude unreliable eye-tracking data. Data gaps of 0.1 s or less were interpolated using MATLAB's shape-preserving cubic spline interpolation (Curve Fitting Toolbox).

After filling the data gaps, the normalised eye-orientation vectors were converted into degrees of horizontal visual angle within the same reference frame as head orientation using Eq. 1³⁰. Positive orientation values indicate a direction to the right of the environmental midline, while negative values indicate a direction to the left. The horizontal gaze direction was determined by combining the transformed horizontal eye-orientation data with the horizontal head orientation data. Due to the data gaps in the eye-orientation data, corresponding data gaps also exist in the gaze direction data. We chose not to fill these gaps using only head orientation data, as the gaze direction is defined as the combination of both horizontal eye and head orientation. For information on the data quality, see supplementary material B.

$$E_{tran} = \frac{\tan^{-1} \left(\frac{EN_{tran}}{EN_{long}} \right)}{\pi} 180^\circ \quad (1)$$

E_{tran} : Horizontal eye-orientation on transverse axis in degrees, EN_{tran} : Normalized eye-orientation on transverse axis, EN_{long} : Normalized eye-orientation on longitudinal axis.

We examined the road user detection and scanning behaviour of individuals with real hemianopia, unimpaired vision, and simulated hemianopia. The road user detection performance was assessed by calculating the time-to-contact at the first moment of braking after the appearance of the road user. The time-to-contact was defined as the time interval, in seconds, between the onset of braking and the estimated time of collision, had the participant not applied the brakes. A time-to-contact of zero indicated that a collision had occurred, while, for example, a time-to-contact of four seconds would indicate that the participant had four seconds remaining before a collision would have occurred at braking initiation. We only include braking onsets that began after the road user appeared in the scene, as braking before road user appearance would not contribute to collision avoidance. The time-to-contact was averaged over all 16 events and separately for predictable events, unpredictable events, events with a distractor absent, and events with a distractor present. Note that our study aims to assess the road-user detection response of individuals with HH while cycling in VR. To achieve this, participants were instructed to respond to crossing road users by applying the hand brakes. Consequently, in this context, time-to-contact reflects the road-user detection response in our participants.

Scanning behaviour was investigated by analysing the changes in horizontal gaze direction and gaze shift behaviour across the participant groups, events types, and in relation to the time-to-contact. Gaze shifts were defined as rapid changes in gaze direction that alter the visual image on the retina. We conducted two analyses: one that assessed scanning behaviour employed throughout the full cycling route and another that focused specifically on the scanning behaviour employed before each event type. The event-related scanning behaviour

was analysed over a period starting ten seconds before road user appearance and ending at the participant's braking onset after road user appearance. Next, the event-related scanning behaviour was averaged separately for predictable events, unpredictable events, events with a distractor absent, and events with a distractor present.

We computed distribution plots that provide the percentage of gaze samples with a specific horizontal gaze direction ranging from -80 to 80 degrees. These plots allow for visually appreciating differences in horizontal gaze direction between participant groups, event-types, and in relation to participants' time-to-contact. In these plots, negative values indicate a gaze direction towards the blind hemispace and positive values indicate a gaze direction towards the visible hemispace. For individuals with unimpaired vision, the blind hemispace was defined as the side of the visual field defect of their age- and gender-matched counterpart with HH. To statistically test for differences in gaze direction, we calculated the variables 'percentage of gaze in the blind hemispace' and the 'interquartile range of the horizontal gaze direction'.

To analyse gaze shift behaviour, we first classified gaze shifts based on the gaze direction data. Gaze shifts were defined as rapid changes in gaze direction that alter the visual image on the retina. For classification, we applied a variable velocity-threshold classifier originally designed to differentiate between slow and fast eye movements³¹. This method has the advantage of distinguishing between rapid shifts in gaze direction and slower, more gradual changes, allowing us to separate gaze shifts from moments of fixation or smooth pursuit of a moving object. Yet, it has the limitation that small gaze shifts may go undetected during high-noise phases caused by bodily movements due to the variable velocity threshold of the gaze shift classifier. Additionally, we observed that the method was less effective in detecting small gaze shifts, probably due to the low sampling frequency, i.e., 40 Hz. Since these smaller shifts provide little new task-relevant information, they are less critical for answering our main questions. Therefore, we only included gaze shifts with an amplitude above 5 degrees in our analysis. Additionally, we unclassified time periods with a low velocity (e.g., fixation or smooth pursuit) that had a duration less than 0.060 s, as fixations and smooth pursuits typically have a longer duration than 0.060s³¹. The amplitude of the remaining gaze shifts was calculated by applying vector summation on the difference in both x and y coordinates (in degrees) between the start and end points of each gaze shift. Next, we computed distribution plots, showing the frequency of occurrence of specific gaze shift amplitudes with bins of 5 degrees, ranging from 5 to 50 degrees. These plots allow for visually appreciating differences in gaze shift behaviour across participant groups, event-types, and in relation to the time-to-contact. The variables used to statistically test for differences in gaze shift behaviour were the frequency of short (< 25 degrees) and long (> 25 degrees) gaze shifts. This cut-off was based on the visualisation of the gaze shift frequency distribution per amplitude and selected to ensure that the outcomes for the frequency of long gaze shifts were not influenced by the higher frequency of short gaze shifts.

Statistical analysis

Statistical analysis was conducted using SPSS (v27 IBM SPSS Statistics, IBM, New York). To assess differences in road user detection performance overall, we performed a univariate ANOVA with the three participant groups (i.e. real HH, unimpaired vision and simulated HH) as between group factor and the dependent variable time-to-contact. To evaluate differences in road user detection performance specific to the event-type, we performed repeated measures ANOVA with the participant group as a between-group factor, the predictability of events as a within-group factor, and the presence of a distractor as a within-group factor. An interaction-effect between event type and participant group was included to assess whether the different event types differently affected the road user detection performance across the participant groups.

To test whether scanning behaviour differs between individuals showing a relatively low or high road user detection performance, we categorised the participants into groups based on their average time-to-contact. For each participant, the time-to-contact values were averaged across all sixteen events. A median split method was used to divide the participants into groups with a relatively long or short time-to-contact, with this division applied separately for each participant group: real HH, unimpaired vision, and simulated HH; see Table 1 for the time-to-contact thresholds.

As previously mentioned, we conducted two distinct analyses to assess differences in scanning behaviour throughout the full cycling route and specifically related to the event types. For the first analyses, we performed univariate ANOVA analyses with the three participant groups (i.e., real HH, unimpaired vision and simulated HH) and the time-to-contact (i.e., relatively long or short) as between-group factors on the scanning variables (i.e., gaze in blind hemispace, horizontal gaze interquartile range, and the frequency of short and long gaze shifts) analysed across the full cycling route. The interaction-effect between participant group and time-to-contact was included to see whether scanning behaviour that may improve road user detection is different between groups. For the second analysis, we performed repeated measures ANOVAs including the participant group as a between-group factor, the predictability of events as a within-group factor, the presence of a distractor as a within-group factor, and the event-related scanning variables (i.e. gaze in blind hemispace, horizontal gaze interquartile range, frequency of (< 25 degrees) and long (> 25 degrees) gaze shifts) as dependent variables.

We did not include the time-to-contact as a between-group factor, as participants were categorised into groups with a relatively long or short time-to-contact based on their average time-to-contact across the full cycling route and not their event-based time-to-contact. Instead, we conducted Spearman correlation analyses between the event-related time-to-contact and scanning variables. For each participant, time-to-contact was averaged over the eight events of each event type (i.e., unpredictable events, predictable events, events with a distractor present, and events without distractors). The correlation analyses were performed for each participant group separately.

Additionally, we performed Spearman correlation analyses between the time-to-contact and the scanning variables (i.e., gaze in blind hemispace, horizontal gaze interquartile range, mean gaze shift amplitude, and mean gaze shift frequency) analysed across the full cycling route for each participant group separately. This analysis

was conducted to ensure reliable interpretation of the results, as dividing participants into groups based on their time-to-contact using the median split method has the disadvantage of discarding the variance in time-to-contact within the groups.

A significance level of 0.05 was adhered to for all analyses. When performing repeated measures ANOVAs, we computed the partial eta squared effect size with 0.01 as small, 0.06 as medium, and 0.14 as large effect size. Correlations above 0.6 were considered strong correlations.

Data availability

The dataset generated and analysed during the current study is available from the corresponding author on reasonable request, under the conditions that the dataset is fully anonymized and with permission of Royal Dutch Visio and the University Medical Center Groningen.

Received: 31 December 2024; Accepted: 25 April 2025

Published online: 29 May 2025

References

1. Bahnmann, M. et al. Compensatory eye and head movements of patients with homonymous hemianopia in the naturalistic setting of a driving simulation. *J. Neurol.* **262**, 316–325. <https://doi.org/10.1007/s00415-014-7554-x> (2015).
2. Bowers, A. R., Ananyev, E., Mandel, A. J., Goldstein, R. B. & Peli, E. Driving with hemianopia: IV. Head scanning and detection at intersections in a simulator. *Invest. Ophthalmol. Vis. Sci.* **55**, 1540–1548. <https://doi.org/10.1167/iovs.13-12748> (2014).
3. Xu, J., Baliutaviciute, V., Swan, G. & Bowers, A. R. Driving with hemianopia X: Effects of cross traffic on gaze behaviors and pedestrian responses at intersections. *Front Hum. Neurosci.* <https://doi.org/10.3389/fnhum.2022.938140> (2022).
4. Swan, G., Savage, S., Zhang, L. & Bowers, A. R. Driving with hemianopia vii: Predicting hazard detection with gaze and head scan magnitude. *Transl. Vis. Sci. Technol.* **10**, 1–16. <https://doi.org/10.1167/tvst.10.1.20> (2021).
5. Papageorgiou, E., Hardiess, G., Mallot, H. A. & Schiefer, U. Gaze patterns predicting successful collision avoidance in patients with homonymous visual field defects. *Vision Res.* **65**, 25–37. <https://doi.org/10.1016/j.visres.2012.06.004> (2012).
6. De Haan, G. A., Melis-Dankers, B. J. M., Brouwer, W. H., Tucha, O. & Heutink, J. The effects of compensatory scanning training on mobility in patients with homonymous visual field defects: A randomized controlled trial. *PLoS ONE* <https://doi.org/10.1371/journal.pone.0134459> (2015).
7. De Haan, G. A., Melis-Dankers, B. J. M., Brouwer, W. H., Tucha, O. & Heutink, J. The effects of compensatory scanning training on mobility in patients with homonymous visual field defects: Further support, predictive variables and follow-up. *PLoS ONE* <https://doi.org/10.1371/journal.pone.0166310> (2016).
8. Postuma, E. M. J. L. et al. A systematic review on visual scanning behaviour in hemianopia considering task specificity, performance improvement, spontaneous and training-induced adaptations. *Disability Rehab.* **46**(15), 3221–3242. <https://doi.org/10.1080/09638288.2023.2243590> (2024).
9. Goettker, A., Borgerding, N., Leeske, L. & Gegenfurtner, K. R. Cues for predictive eye movements in naturalistic scenes. *J. Vis.* **23**(10), 12. <https://doi.org/10.1167/jov.23.10.12> (2023).
10. Muttart, J. W., Fisher, D. L., Pollatsek, A. P. & Marquard, J. Comparison of Anticipatory Glancing and Risk Mitigation of Novice Drivers and Exemplary Drivers when Approaching Curves. *Driving Assessment Conference 7*; <https://doi.org/10.17077/drivingassessment.1490>.
11. Divekar, G., Pradhan, A., Pollatsek, A. & Fisher, D. Effect of external distractions: Behavior and vehicle control of novice and experienced drivers evaluated. *Transp. Res. Rec.* <https://doi.org/10.3141/2321-03> (2012).
12. Lee, S., Black, A. A., Lacherez, P. & Wood, J. M. Eye movements and road hazard detection: Effects of blur and distractors. *Optometry Vis. Sci.* <https://doi.org/10.1097/OPX.0000000000000903> (2016).
13. Edquist, J., Horberry, T., Hosking, S. & Johnston, I. Effects of advertising billboards during simulated driving. *Appl. Ergon.* **42**, 619–626. <https://doi.org/10.1016/j.apergo.2010.08.013> (2011).
14. Biebl, B., Arcidiacono, E., Kacianka, S., Rieger, J. W. & Bengler, K. Opportunities and limitations of a gaze-contingent display to simulate visual field loss in driving simulator studies. *Frontiers Neuroergonom.* <https://doi.org/10.3389/fnrgo.2022.916169> (2022).
15. Tant, M. L. M., Cornelissen, F. W., Kooijman, A. C. & Brouwer, W. H. Hemianopic visual field defects elicit hemianopic scanning. *Vis. Res.* **42**(10), 1339–1348. [https://doi.org/10.1016/s0042-6989\(02\)00044-5](https://doi.org/10.1016/s0042-6989(02)00044-5) (2002).
16. Michon, J. A. A critical view of driver behavior models: What do we know, what should we do? In *Human behavior and traffic safety* (eds Evans, L. & Schwing, R. C.) 485–524 (Springer US, Boston, MA, 1986). https://doi.org/10.1007/978-1-4613-2173-6_19.
17. Jelijs, B., Heutink, J., de Waard, D., Brookhuis, K. A. & Melis-Dankers, B. J. M. Compensatory behaviour of visually impaired cyclists in everyday settings. *Transp. Res. Part F Traffic Psychol. Behav.* **87**, 138–148. <https://doi.org/10.1016/j.trf.2022.04.003> (2022).
18. Nowakowska, A., Clarke, A. D. F., Sahraie, A. & Hunt, A. R. Practice-related changes in eye movement strategy in healthy adults with simulated hemianopia. *Neuropsychologia* **128**, 232–240. <https://doi.org/10.1016/j.neuropsychologia.2018.01.020> (2019).
19. Schuett, S., Kentridge, R. W., Zihl, J. & Heywood, C. A. Are hemianopic reading and visual exploration impairments visually elicited? New insights from eye movements in simulated hemianopia. *Neuropsychologia* **47**, 733–746. <https://doi.org/10.1016/j.neuropsychologia.2008.12.004> (2009).
20. Kasneci, E. et al. Driving with binocular visual field loss? A study on a supervised on-road parcours with simultaneous eye and head tracking. *PLoS ONE* <https://doi.org/10.1371/journal.pone.0087470> (2014).
21. Postuma, E. M. J. L., de Haan, G. A., Heutink, J. & Cornelissen, F. W. Virtual street crossing and scanning behavior in people with hemianopia: a step towards successful crossings. *J. Vision (In Press)* (2025).
22. Shahar, A., Alberti, C. F., Clarke, D. & Crundall, D. Hazard perception as a function of target location and the field of view. *Accid. Anal. Prev.* **42**, 1577–1584. <https://doi.org/10.1016/j.aap.2010.03.016> (2010).
23. Drewes, J., Feder, S. & Einhäuser, W. Gaze during locomotion in virtual reality and the real world. *Front Neurosci.* <https://doi.org/10.3389/fnins.2021.656913> (2021).
24. Berton, F., Olivier, A. H., Bruneau, J., Hoyet, L., & Pettre, J. Studying gaze behaviour during collision avoidance with a virtual walker: Influence of the virtual reality setup. *IEEE Conference on Virtual Reality and 3D User Interfaces (VR)*. 717–72; <https://doi.org/10.1109/VR.2019.8798204> (2019).
25. Pfeil, K., Taranta, E. M., Kulshreshtha, A., Wisniewski, P. & LaViola, J. J. A comparison of eye-head coordination between virtual and physical realities. In: *Proceedings—ACM Symposium on Applied Perception*; <https://doi.org/10.1145/3225153.3225157> (2018).
26. Iorizzo, D. B., Riley, M. E., Hayhoe, M. & Huxlin, K. R. Differential impact of partial cortical blindness on gaze strategies when sitting and walking—An immersive virtual reality study. *Vis. Res.* **51**, 1173–1184. <https://doi.org/10.1016/j.visres.2011.03.006> (2011).
27. Folstein, M. F., Folstein, S. E. & McHugh, P. R. Mini-mental state. *J. Psychiatric Res.* **12**(3), 189–198. [https://doi.org/10.1016/0022-3956\(75\)90026-6](https://doi.org/10.1016/0022-3956(75)90026-6) (1975).

28. Bos, J. E., MacKinnon, S. N. & Patterson, A. Motion sickness symptoms in a ship motion simulator: Effects of inside, outside, and no view. *Aviat. Space Environ. Med.* **76**(12), 1111–1118 (2005).
29. Kennedy, R. S., Lane, N. E., Berbaum, K. S. & Lilienthal, M. G. Simulator sickness questionnaire: An enhanced method for quantifying simulator sickness. *Int. J. Aviation Psychol.* **3**(3), 203–220 (1993).
30. Imaoka, Y., Flury, A. & de Bruin, E. D. Assessing saccadic eye movements with head-mounted display virtual reality technology. *Front Psychiatry* <https://doi.org/10.3389/fpsy.2020.572938> (2020).
31. Hooge, I. & Camps, G. Scan path entropy and arrow plots: Capturing scanning behavior of multiple observers. *Frontiers Psychol.* <https://doi.org/10.3389/fpsyg.2013.00996> (2013).

Acknowledgements

The authors would like to thank all individuals who participated in this study. Additionally, we express our gratitude towards the bachelor and master students, who assisted in collecting the data. We used ChatGPT for revising sentences, improving grammar and enriching the vocabulary of this text. This project was funded by the Visio Foundation, Amsterdam, The Netherlands. The contribution of EP, GH, and JH was also partially supported by ZonMw program Expertisefunctie Zintuiglijk Gehandicapt [grant number 637005001].

Author contributions

All authors contributed to the development of the virtual environment, experimental protocol, and writing the manuscript. Author E.P. collected the data, created the data analysis script, analysed the data, wrote the main text, and prepared the figures and tables. Authors G.H., F.C. and J.H. reviewed the manuscript.

Declarations

Competing interests

All authors declare to have no competing interests.

Additional information

Supplementary Information The online version contains supplementary material available at <https://doi.org/10.1038/s41598-025-00212-1>.

Correspondence and requests for materials should be addressed to G.A.H.

Reprints and permissions information is available at www.nature.com/reprints.

Publisher's note Springer Nature remains neutral with regard to jurisdictional claims in published maps and institutional affiliations.

Open Access This article is licensed under a Creative Commons Attribution-NonCommercial-NoDerivatives 4.0 International License, which permits any non-commercial use, sharing, distribution and reproduction in any medium or format, as long as you give appropriate credit to the original author(s) and the source, provide a link to the Creative Commons licence, and indicate if you modified the licensed material. You do not have permission under this licence to share adapted material derived from this article or parts of it. The images or other third party material in this article are included in the article's Creative Commons licence, unless indicated otherwise in a credit line to the material. If material is not included in the article's Creative Commons licence and your intended use is not permitted by statutory regulation or exceeds the permitted use, you will need to obtain permission directly from the copyright holder. To view a copy of this licence, visit <http://creativecommons.org/licenses/by-nc-nd/4.0/>.

© The Author(s) 2025